http://dx.doi.org/10.1090/conm/218/02999

Contemporary Mathematics
Volume **218**, 1998
B 0-8218-0988-1-02999-X

Nonmatching Grids for Fluids

Yves Achdou, Gassan Abdoulaev, Jean-Claude Hontand,
Yuri A. Kuznetsov, Olivier Pironneau, and Christophe Prud'homme

1. Introduction

We review some topics about the use of nonmatching grids for fluids. In a first part, we discuss the mortar method for a convection diffusion equation. In a second part, we present a three dimensional Navier-Stokes code, based on mortar elements, whose main ingredients are the method of characteristics for convection, and a fast solver for elliptic equations for incompressibility. Finally, preliminary numerical results are given.

Since the late nineteen eighties, interest has developed in non-overlapping domain decomposition methods coupling different variational approximations in different subdomains. The *mortar element methods*, see [**10**], [**28**], have been designed for this purpose and they allow us to combine different discretizations in an optimal way. Optimality means that the error is bounded by the sum of the subregion-by-subregion approximation errors without any constraints on the choice of the different discretizations. One can, for example couple spectral methods with finite elements, or different finite element methods with different meshes.

The advantages of the mortar method are:

- It permits to use spectral methods with flexibility.
- It is well suited for partial differential equations involving highly heterogeneous media.
- Mesh adaption can be made local [**9**].
- It enables one to assemble several meshes generated independently: this is important, since constructing meshes is not an easy problem in three dimensions.
- In the finite elements context, it permits the use of locally structured grids in the subdomains, thence fast local solvers. Besides, for computational fluid dynamics, structured grids are very helpful in boundary layers for instance.
- It permits the use of sliding meshes see [**6**].

1991 *Mathematics Subject Classification.* Primary 65M55; Secondary 76D05, 65M60, 65N55.

The second and fourth authors were partially supported by French-Russian Liapunov Institute for Informatics and Applied Mathematics and INRIA. This work was partially carried out at the CEMRACS summer school, http://www.asci.fr/cemracs. The first author was partially supported by CNRS PICS 478. The computations were performed on the Cray T3E at IDRIS, Orsay, France.

In this paper, we focus on the use of the mortar method for the simulation of fluid dynamics problems.

After reviewing the method for symmetric problems, we propose and analyze a mortar method suited for convection-diffusion problems. We show that upwinding terms should be added at the interfaces between subdomains.

Then, we discuss a 3D Navier-Stokes code with nonmatching grids, which is being developed at laboratory ASCI (Applications Scientifiques du Calcul Intensif) in Orsay(France). This code is based on a projection-characteristics scheme [**4**] and on a fast parallel solver for the pressure. With such a scheme, the involved elliptic operators are time-invariant and symmetric. The solver we use for the pressure has been developed in [**22**] and tested in [**1**]. It is used for solving the saddle point linear system arising from the mortar element discretization of the pressure equation. Other solvers or preconditioners have been developed for nonmatching grid problems, *e.g* substructuring preconditioners in the space of weakly continuous functions [**14, 5, 16**], or Neumann-Neumann preconditioners [**23**].

Finally, we present some results both in 2D and 3D. The 2D results are also obtained with a mortar element method, but with a vorticity stream-function formulation. The 3D results are preliminary, since the code is in progress.

2. A brief review on the mortar method

Assume that we have to solve the elliptic problem: find $u \in H^1(\Omega)$ such that

$$\tilde{a}(u,v) = (f,v), \quad \forall v \in H^1(\Omega) \tag{1}$$

in a two dimensional domain Ω, where $\tilde{a}(\cdot,\cdot)$ is a second order bilinear form, continuous on $H^1(\Omega)$. We shall assume for simplicity that $\tilde{a}(u,v) = \int_\Omega \nabla u \cdot \nabla v$, which corresponds to a Neumann problem, and that the right hand side f is such that (1) has a solution, unique up to the addition of constants. Consider a nonoverlapping domain decomposition $\overline{\Omega} = \bigcup_{k=1}^{K} \overline{\Omega}_k$. We assume that each subdomain Ω_k is a piecewise regular, curved polygon. For simplicity only we also suppose that the domain decomposition is geometrically conforming. It means that if $\gamma_{kl} = \overline{\Omega}_k \cap \overline{\Omega}_l \quad (k \neq l)$ and $\gamma_{kl} \neq \emptyset$, then γ_{kl} can be either a common vertex of Ω_k and Ω_l, or a common edge, or a common face. In the last case we define $\Gamma_{kl} = \gamma_{kl}$ as the interface between Ω_k and Ω_l. Note that $\Gamma_{kl} = \Gamma_{lk}$. The union Γ of all $\partial\Omega_k \backslash \partial\Omega$ is called the skeleton (or interface) of the decomposition.

Let us introduce the spaces $X_k \equiv H^1(\Omega_k)$. It is also possible to define the local bilinear forms a_k on $X_k \times X_k$ by $a_k(u_k, v_k) = \int_{\Omega_k} \nabla u_k \cdot \nabla v_k$, and the global bilinear form

$$a : \prod_{k=1}^{K} X_k \times \prod_{k=1}^{K} X_k \to \mathbb{R}, \quad a(u,v) = \sum_{k=1}^{K} a_k(u_k, v_k). \tag{2}$$

Suppose that each Ω_k is provided with its own discretization $X_{k,h}$ of X_k. In what follows, the discrete spaces are of finite element type, but the proposed method can also be used for any discretization of the variational problem. To derive a global discretization of $H^1(\Omega)$, yielding an accurate Galerkin approximation of (1), the mortar element method was introduced in [**10**]. Reviewing the basics of the method, the global discrete space is a subspace of $X_h \equiv \prod_{1 \leq k \leq K} X_{k,h}$ obtained by imposing matching conditions on each face Γ_{kl}. On any such face, there are two

values, the traces v_k (respectively v_l) of a function defined in Ω_k (respectively Ω_l). For $k < l$ such that $|\partial\Omega_l \cap \partial\Omega_k| > 0$, denote by $\widetilde{W}_{k,l,h}$ (respectively $\widetilde{W}_{l,k,h}$) the trace of the finite element space $X_{k,h}$ (respectively $X_{l,h}$) on Γ_{kl}. Let $W_{k,l,h}$ be a subspace of codimension two of either $\widetilde{W}_{k,l,h}$ or $\widetilde{W}_{l,k,h}$. We refer to [**10**] for more details and the exact definition of this subspace. We then set

$$Y_h \equiv \left\{ \begin{array}{l} \mathbf{v} \in X_h : \text{ for all } k < l \text{ such that } |\partial\Omega_l \cap \partial\Omega_k| > 0, \\ \int_{\Gamma_{kl}} (v_k - v_l)\psi = 0, \quad \forall \psi \in W_{k,l,h} \end{array} \right\}. \tag{3}$$

The discrete problem reads: find $u_h \in Y_h$ such that

$$\forall v_h \in Y_h, \quad a(u_h, v_h) = \int_\Omega f v_h. \tag{4}$$

It has been established in [**10**] that the resulting discretization error is as good as for comparable conforming finite element or spectral approximations. Indeed, if the solution of (1) is regular enough (in $H^{\frac{3}{2}+\epsilon}$) then the error in the norm $\|v\|_{1,*} \equiv \sqrt{a(v,v)}$ is bounded by a constant time the sum of the subregion by subregion best approximation errors.

3. The mortar method for convection-diffusion problems

In this section, we present a mortar method suited for non symmetric problems. Since this method is only studied theoretically here and is not implemented in our Navier-Stokes code, this section can be seen as a digression. Let us consider the stationary scalar linear convection dominated convection-diffusion equation:

$$\begin{array}{ll} -\epsilon\Delta u + \nabla \cdot (\beta u) + \sigma u = f & \text{in } \Omega, \\ u = g & \text{on } \partial\Omega, \end{array} \tag{5}$$

where Ω is a bounded polygonal domain in $\mathbb{R}^2$, σ and ϵ are two constants, ϵ being small. It is assumed that the velocity β is smooth and that $\sigma - \frac{1}{2}|\nabla \cdot \beta| > \bar{\sigma} > 0$. In the following, we take $g = 0$ in (5).

If optimal error estimates are desired, the mortar method reviewed above cannot be applied in a straightforward manner. We shall show that upwinding terms are needed at the interfaces between subdomains.

In this section, we work with triangular meshes in the subdomains and P_1 elements and we assume that the triangulations in the subdomains are regular and quasi uniform. Let h_k be the maximal diameter of the triangles in Ω_k. We shall assume that $\epsilon \ll h_k$. In this case, introducing upwinding by using *e.g.* streamline diffusion methods, see [**20**], is necessary because a standard Galerkin approach for discretizing (5) would produce oscillations.

We denote by X_{kh} the space of continuous and piecewise linear functions on the triangulation of Ω_k, vanishing on $\partial\Omega_k \cap \partial\Omega$, and Y_h is defined as in (3).

Consider a family $(\delta_k)_{1 \le k \le K}$ of small positive parameters : $\delta_k \sim h_k$ and the non symmetric bilinear form a_k $X_k \times X_k \to \mathbb{R}$:

$$a_k(u_k, v_k) = \epsilon \int_{\Omega_k} \nabla u_k \cdot \nabla v_k + \int_{\Omega_k} (\sigma u_k + \nabla \cdot (\beta u_k))(v_k + \delta_k \nabla \cdot (\beta v_k)). \tag{6}$$

It corresponds to a streamline diffusion method applied in subdomain Ω_k, see [**20**]. However, the discrete problem: find $u_h \in Y_h$ such that

$$\forall v_h \in Y_h, \quad a(u_h, v_h) = \sum_{k=1}^{K} \int_{\Omega_k} f(v_{kh} + \delta_k \nabla \cdot (\beta v_{kh})) \tag{7}$$

with

$$a(u, v) = \sum_{k=1}^{K} a_k(u_k, v_k) \tag{8}$$

would not necessarily yield optimal error estimates. Indeed,

$$\begin{array}{l} a(u,u) = \\ \sum_{1\le k\le K} \int_{\Omega_k} \epsilon|\nabla u_k|^2 + (\sigma + \frac{1}{2}\nabla\cdot\beta)u_k^2 + h_k|\nabla\cdot(\beta u_k)|^2 + \sigma h_k \nabla\cdot(\beta u_k)u_k \\ + \frac{1}{2}\sum_{|\Gamma_{kl}|\neq 0} \int_{\Gamma_{kl}} \beta.n_{kl}(u_k^2 - u_l^2) \end{array} \tag{9}$$

and it is not possible to control the term

$$\frac{1}{2} \sum_{|\Gamma_{kl}|\neq 0} \int_{\Gamma_{kl}} \beta.n_{kl}(u_k^2 - u_l^2)$$

in an optimal way. Therefore, we shall also introduce a stabilizing term for each interface Γ_{kl}: for $k < l$: $|\Gamma_{kl}| \neq 0$, let us define the bilinear form $\tilde{a}_{kl}$: $(X_k \times X_l)^2 \to \mathbb{R}$:

$$\tilde{a}_{kl}(u_k, u_l, v_k, v_l) = \int_{\Gamma_{kl}} (\beta \cdot n_{kl})^-(u_k - u_l)v_k + \int_{\Gamma_{kl}} (\beta \cdot n_{lk})^-(u_l - u_k)v_l, \tag{10}$$

where x^- denotes the negative part of x: $x^- = \frac{1}{2}(|x| - x)$. The bilinear form a:$X \times X \to \mathbb{R}$ is now defined by

$$a(u, v) = \sum_{1\le k\le K} a_k(u_k, v_k) + \sum_{k<l\,:\,|\Gamma_{kl}|\neq 0} \tilde{a}_{kl}(u_k, u_l, v_k, v_l). \tag{11}$$

The chosen discretization of (5) is: find $u_h \in Y_h$ such that

$$\forall v_h \in Y_h, \quad a(u_h, v_h) = \sum_{1\le k\le K} \int_{\Omega_k} f(v_{kh} + \delta_k \nabla \cdot (\beta v_{kh})). \tag{12}$$

REMARK 1. Note that the upwinding is done by the streamline diffusion method inside the subdomains, and by some discontinuous Galerkin like method at the interfaces between subdomains, where no strong continuity is available.

Let $\|v\|$ denotes the broken norm :

$$\|v\|^2 \equiv \sum_{1\le k\le K} \left\{ \epsilon \int_{\Omega_k} |\nabla v_k|^2 + \frac{\bar{\sigma}}{2} \int_{\Omega_k} v_k^2 + \frac{\delta_k}{2} \int_{\Omega_k} (\nabla \cdot (\beta v_k))^2 \right\}, \tag{13}$$

and $|v|$ the semi-norm

$$|v|^2 \equiv \frac{1}{2} \sum_{k<l\,:\,|\Gamma_{kl}|\neq 0} \int_{\Gamma_{kl}} |\beta \cdot n_{kl}|(v_k - v_l)^2 \tag{14}$$

We will prove an error estimate in the following norm :

$$|||v||| \equiv \left(\|v\|^2 + |v|^2 \right)^{\frac{1}{2}}. \tag{15}$$

The stability of the method stems from the following lemma:

LEMMA 2. *If* $\forall k \in \{1, K\}, \quad \delta_k \leq \frac{\bar{\sigma}}{2\sigma^2}$, *then for any* $v \in Y_h$,

$$a(v, v) \geq |||v|||^2. \tag{16}$$

From this lemma and from the best fit estimate in the L^2-norm when approaching a sufficiently regular function by a function in Y_h (see [**8**]), we obtain the following result, which states that optimal error estimates are obtained, similarly as for the conforming case.

PROPOSITION 3. *Assume that the solution of (5) is in* $H_0^1(\Omega) \cap \prod_{1 \leq k \leq K} H^2(\Omega_k)$ *and that*

$$\forall k \in \{1, K\}, \quad \epsilon \leq ch_k \quad \text{and} \quad \delta_k = h_k, \tag{17}$$

then there exists a constant C *such that, if* u_h *is the solution of (12),*

$$|||u - u_h||| \leq C \sum_{1 \leq k \leq K} h_k^{\frac{3}{2}} \|u_k\|_{H^2(\Omega_k)}. \tag{18}$$

PROOF. It is seen from [**10**], [**8**] (see in particular [**8**], remark 7), that there exists $\tilde{u}_h$ in Y_h such that $w_h = u - \tilde{u}_h$ satisfies

$$\left(\sum_{1 \leq k \leq K} \int_{\Omega_k} |\nabla w_{kh}|^2 \right)^{\frac{1}{2}} \leq C \sum_{1 \leq k \leq K} h_k \|u_k\|_{H^2(\Omega_k)} \tag{19}$$

and

$$\left(\sum_{1 \leq k \leq K} \int_{\Omega_k} w_{kh}^2 \right)^{\frac{1}{2}} \leq C \sum_{1 \leq k \leq K} h_k^2 \|u_k\|_{H^2(\Omega_k)}. \tag{20}$$

These approximations results have been obtained when proving that the mortar method leads to optimal error estimates for an elliptic problem. Choosing other jump condition on interface, *i.e.* other spaces Y_h often lead to poorer approximation results (see [**10**]). Therefore, from assumption (17) ,

$$|||w_h||| \leq C \sum_{1 \leq k \leq K} h_k^{\frac{3}{2}} \|u_k\|_{H^2(\Omega_k)}. \tag{21}$$

Let $\tilde{e}_h = \tilde{u}_h - u_h$ and $e_h = u - u_h$. From (5) and (12) one obtains that

$$a(e_h, \tilde{e}_h) = \epsilon \sum_{1 \leq k \leq K} \delta_k \int_{\Omega_k} \Delta u \nabla.(\beta \tilde{e}_{kh}) + \epsilon \sum_{k<l \,:\, |\Gamma_{kl}| \neq 0} \int_{\Gamma_{kl}} \frac{\partial u}{\partial n_{kl}} (\tilde{e}_{kh} - \tilde{e}_{lh}). \tag{22}$$

Therefore since $\tilde{e}_h = e_h - w_h$,

$$\begin{aligned} &|||e_h|||^2 \\ &= a(e_h, w_h) + \\ &\epsilon \sum_{1 \leq k \leq K} \delta_k \int_{\Omega_k} \Delta u \nabla.(\beta(e_{kh} - w_{kh})) + \epsilon \sum_{k<l \,:\, |\Gamma_{kl}| \neq 0} \int_{\Gamma_{kl}} \frac{\partial u}{\partial n_{kl}} (\tilde{e}_{kh} - \tilde{e}_{lh}). \end{aligned} \tag{23}$$

The last two terms are consistency errors. Using arguments very similar to those of [**20**], it can be proved that

$$|a(e_h, w_h)| \leq C|||e_h||| \sum_{1 \leq k \leq K} h_k^{\frac{3}{2}} \|u_k\|_{H^2(\Omega_k)}. \tag{24}$$

It can also be seen that

$$
\begin{aligned}
&\epsilon \left| \sum_{1\leq k\leq K} \delta_k \int_{\Omega_k} \Delta u \nabla.(\beta(e_{kh} - w_{kh})) \right| \\
&\leq \epsilon \|\Delta u\|_{L^2(\Omega)} \sum_{1\leq k\leq K} \delta_k \|\nabla.(\beta(e_{kh}\|_{L^2(\Omega_k)} + \delta_k \|\nabla.(\beta(w_{kh}\|_{L^2(\Omega_k)} \\
&\leq C \left(|||e_h||| + \sum_{1\leq k\leq K} h_k^{\frac{3}{2}} \|u_k\|_{H^2(\Omega_k)} \right) \sum_{1\leq k\leq K} h_k^{\frac{3}{2}} \|u_k\|_{H^2(\Omega_k)}.
\end{aligned} \tag{25}
$$

Finally, since $\tilde{e} \in Y_h$, calling π_h the L^2 projection on W_h (see [**10**]),

$$
\epsilon \left| \int_{\Gamma_{kl}} \frac{\partial u}{\partial n_{kl}} (\tilde{e}_{kh} - \tilde{e}_{lh}) \right| = \epsilon \left| \int_{\Gamma_{kl}} (I - \pi_h) \frac{\partial u}{\partial n_{kl}} (\tilde{e}_{kh} - \tilde{e}_{lh}) \right|, \tag{26}
$$

and using the lemma 4.1 of [**10**],

$$
\begin{aligned}
&\epsilon \left| \sum_{k<l \,:\, |\Gamma_{kl}|\neq 0} \int_{\Gamma_{kl}} \frac{\partial u}{\partial n_{kl}} (\tilde{e}_{kh} - \tilde{e}_{lh}) \right| \\
&\leq C \left(|||e_h||| + \sum_{1\leq k\leq K} h_k^{\frac{3}{2}} \|u_k\|_{H^2(\Omega_k)} \right) \sum_{1\leq k\leq K} h_k^{\frac{3}{2}} \|u_k\|_{H^2(\Omega_k)}.
\end{aligned} \tag{27}
$$

Collecting all the above estimates yields the desired result. □

Such a discretization can be generalized to nonlinear conservation laws, see [**3**]:

$$
\begin{aligned}
-\epsilon \Delta u + \nabla \cdot f(u) + \sigma u &= d \qquad \text{in } \Omega \\
u &= 0 \qquad \text{on } \partial\Omega.
\end{aligned} \tag{28}
$$

As above, one must add a flux term on the interfaces

(29)

$$
a_{kl}(u_k, u_l, v_k, v_l) = -\int_{\Gamma_{kl}} n_{kl} \cdot (f(u_k)v_k - f(u_l)v_l) + \int_{\Gamma_{kl}} n_{kl} \cdot g(u_k, u_l)(v_k - v_l)
$$

where $n_{kl} \cdot (g(u_k, u_l)$ is a Godunov flux:

$$
n_{kl} \cdot g(u_k, u_l) = \min_{u_k \leq u \leq u_l} n_{kl} \cdot f(u) \quad \text{if } u_k \leq u_l.
$$

One can choose instead an Osher flux:

$$
n_{kl} \cdot g(u_k, u_l) = \frac{1}{2} n_{kl} \cdot (f(u_k) + f(u_l)) + \frac{1}{2} \int_{(u_k, u_l)} |n_{kl} \cdot f'(u)|.
$$

4. A Navier Stokes solver using the mortar element method

Getting back to what we have implemented, the proposed scheme is based on both projection and the characteristic Galerkin methods. As we shall see, the main advantage of such a scheme is that

- Thanks to the characteristics methods, the linear problems solved at each time step involve time invariant and symmetric elliptic operators.
- Thanks to the projection method, the problems for pressure and velocities are decoupled since the linearized Stokes problem is not solved exactly.

The code is implemented in three dimensions and is based on a fast solver for the pressure, which shall also be reviewed in this section. We shall also present 2D results with a mortar method, but the 2D code is based on a stream function-vorticity formulation.

In the following, we consider the time-dependent Navier–Stokes problem in which homogeneous Dirichlet condition has been assumed for simplicity. For a given body force f (possibly dependent on time) and a given divergence-free initial velocity field u_0, find a velocity field u and a pressure field p such that $u = u_0$ at $t = 0$, and for $t > 0$,

$$\begin{aligned} &\frac{\partial u}{\partial t} - \nu\Delta u + (u\cdot\nabla)u + \nabla p = f \quad \text{in } \Omega\times(0,T),\\ &\nabla\cdot u = 0 \quad \text{in } \Omega\times(0,T),\\ &u = 0 \quad \text{on } \partial\Omega\times(0,T). \end{aligned} \tag{30}$$

4.1. The scheme.

4.1.1. *The Galerkin characteristics method.* As in [**25**],[**27**], the total time derivatives are approximated by a finite difference formula in space and time, leading to a Eulerian-Lagrangian method: $\frac{Du}{Dt} = \frac{\partial u}{\partial t} + u\cdot\nabla u$ is discretized by

$$\frac{1}{\delta t}(u^{m+1} - u^m \circ X^m),$$

where $X^m(x)$ is the solution at time t^m of the backward Cauchy problem:

$$\frac{dX^m}{d\tau}(x,\tau) = u^m(X^m(x,\tau)) \quad \tau\in[t^m, t^{m+1}], \tag{31}$$

$$X^m(x,t^{m+1}) = x. \tag{32}$$

It can be seen easily that

$$w^m \circ X^m(x,t^m) \approx w^m(x - \delta t u^m(x)).$$

Therefore, at each time step, if we did not combine the characteristics method with a projection scheme, we would have to solve the linearized Stokes problem

$$\frac{1}{\delta t}(u^{m+1} - u^m\circ X^m(x,t^m)) - \nu\delta u^{m+1} + \nabla p^{n+1} = 0, \quad \text{in } \Omega \tag{33}$$

$$\nabla\cdot u^{n+1} = 0 \quad \text{in } \Omega. \tag{34}$$

4.1.2. *The spatial discretization.* We introduce $\tilde{V}_h$ and Y_h two mortar finite element approximations of $(H_0^1(\Omega))^3$ and $L^2(\Omega)$. For instance, we can take a mortar version of the Q_1 iso Q_2, Q_1 method: if the subdomains Ω_k are meshed with hexahedrons, and if the functions of $X_{k,h}$ are continuous and piecewise polynomial of degree 1 in each variable (Q_1), the space Y_h is given by (3). Then the mortar space $\tilde{V}_h$ is composed of the Q_1 functions on the finer mesh (obtained by dividing each hexahedron of the initial mesh into eight hexahedra), vanishing on $\partial\Omega$ and matched at subdomains interfaces with a corresponding mortar condition.

We assume that the two spaces satisfy the Babuška-Brezzi inf-sup condition [**12, 7**]: there exists $c > 0$ such that

$$\inf_{q_h\in Y_h}\sup_{v_h\in\tilde{V}_h}\frac{\sum_{k=1}^K\int_{\Omega_k} v_{kh}\cdot\nabla q_{kh}}{\|v_h\|_{1,*}\|q_h\|_0} \geq c.$$

We now introduce a discrete divergence operator $C_h : \tilde{V}_h \longrightarrow Y_h$ and its transpose $C_h^T : Y_h \longrightarrow \tilde{V}_h'$ as follows: for every couple (v_h, q_h) in $\tilde{V}_h \times Y_h$ we have

$$(C_h v_h, q_h) = \sum_{k=1}^{K} \int_{\Omega_k} v_{kh} \cdot \nabla q_{kh} = (v_h, C_h^T q_h). \tag{35}$$

Calling $A_h : \tilde{V}_h \longrightarrow \tilde{V}_h'$ the stiffness operator for the velocity

$$(A_h v_h, w_h) = \frac{1}{\delta t} \sum_{k=1}^{K} \int_{\Omega_k} v_{kh} w_{kh} + \nu \sum_{k=1}^{K} \int_{\Omega_k} \nabla v_{kh} \cdot \nabla w_{kh},$$

the discrete Stokes problem at time t^{m+1} reads:

$$A_h v_h^{m+1} + C_h^T q_h^{m+1} = g^{m+1} \tag{36}$$

$$C_h v_h^{m+1} = 0, \tag{37}$$

where g^{m+1} is computed from $u^m \circ X^m(x, t^m)$.

4.1.3. *The characteristic-projection scheme.* The projection method was introduced in [**15**] and [**29**]. It consists of using two approximations for the velocity at time step t^{m+1} namely u_h^{m+1} and $\tilde{u}_h^{m+1}$. The approximation $\tilde{u}_h^{m+1}$ is sought in the previously defined space $\tilde{V}_h$. The second approximation u_h^{m+1} belongs to the space

$$V_h \equiv \tilde{V}_h + \tilde{\nabla} Y_h, \tag{38}$$

where the operator $\tilde{\nabla}$ is defined by:

$$\tilde{\nabla} : Y_h \to \prod_{k=1}^{K} (L^2(\Omega_k))^3 \tag{39}$$

$$\tilde{\nabla} v_h = (\nabla v_{1h}, \ldots, \nabla v_{Kh}). \tag{40}$$

It is possible to extend the operator C_h by D_h: $D_h : V_h \longrightarrow Y_h$:

$$(D_h v_h, q_h) = \sum_{k=1}^{K} \int_{\Omega_k} v_{kh} \cdot \nabla q_{kh} \tag{41}$$

and to define D_h^T by $(v_h, D_h^T q_h) = (D_h v_h, q_h)$.

We are now interested in defining a projection/Lagrange-Galerkin scheme. We define two sequences of approximate velocities $\{\tilde{u}_h^m \in \tilde{V}_h\}$ and $\{u_h^m \in V_h\}$ and one sequence of approximate pressures $\{p_h^m \in Y_h\}$ as follows:

- **Initialization**: the sequences $\{u_h^m\}$, $\{\tilde{u}_h^m\}$ are initialized by for example $u_h^0 = \tilde{u}_h^0 = \hat{u}_h^0$ and the sequence $\{p_h^m\}$ is initialized by $p_h^0 = \hat{p}_h^0$.
- **Time loop**: For $0 \leq m$, solve

$$(A_h \tilde{u}_h^{m+1}, v_h) - (\frac{u_h^m}{\delta t}, v_h) + (\frac{\tilde{u}_h^m - \tilde{u}_h^m(X_h^m)}{\delta t}, v_h) = (f(t^{m+1}), v_h), \quad \forall v_h \in \tilde{V}_h, \tag{42}$$

and

$$\frac{u_h^{m+1} - \tilde{u}_h^{m+1}}{\delta t} + D_h^T p_h^{m+1} = 0, \quad D_h u_h^{m+1} = 0. \tag{43}$$

The velocity u_h^{m+1} can be seen as the L^2 projection of $\tilde{u}_h^{m+1}$ on the space of discrete divergence free functions. It satisfies only a weak non penetration condition at the boundary.

In practice, the projected velocity u_h^m must be eliminated from the algorithm as follows (see Rannacher [**26**] or Guermond [**19**]). For $m \geq 1$, replace u_h^m in (42) by its definition which is given by (43) at the time step t^m. In (43), u_h^{m+1} is eliminated by applying D_h to the first equation and by noting that D_h is an extension of C_h. If by convention we set $p_h^{-1} = \hat{p}_h^0$, the algorithm which should be implemented in practice reads for $m \geq 0$:

$$(44) \quad (A\tilde{u}_h^{m+1}, v_h) + (C_h^T p_h^m, v_h) = (f(t^{m+1}), v_h) + (\frac{\tilde{u}_h^m(X_h^m)}{\delta t}, v_h) \qquad \forall v_h \in \tilde{V}_h,$$

and

$$(45) \qquad (D_h D_h^T p_h^{m+1}, q_h) = (\frac{C_h \tilde{u}_h^{m+1}}{\delta t}, q_h) \qquad \forall q_h \in Y_h.$$

Thanks to the choice of the space V_h (38) and of discretization for the divergence operator (41), the projection step can be rewritten: find p_h^{m+1} in Y_h such that

$$(46) \qquad \forall q_h \in Y_h, \quad \sum_{k=1}^{K} \int_{\Omega_k} \nabla p_{kh}^{m+1} \cdot \nabla q_{kh} = \frac{1}{\delta t} \sum_{k=1}^{K} \int_{\Omega_k} \tilde{u}_{kh}^{m+1} \cdot \nabla q_{kh},$$

which is exactly the mortar discretization of the Poisson problem (1).

This algorithm has been analyzed for conforming discretizations (no mortars) in [**4**]. Roughly speaking, the results are the following: It is shown that provided the time step is of $\mathcal{O}(h^{d/4})$, where h is the mesh size and d is the space dimension $(2 \leq d \leq 3)$, the proposed method yields for finite time T an error of $\mathcal{O}(h^{l+1} + \delta t)$ in the L^2 norm for the velocity and an error of $\mathcal{O}(h^l + \delta t)$ in the H^1 norm (or the L^2 norm for the pressure), where l is the spatial discretization order, if the solution is regular enough.

Second order schemes in time can also be implemented.

4.1.4. *The projection method as a preconditioner.* As shown by Cahouet and Chabard [**13**], Guermond[**19**], or Turek [**30**], the ingredients used by the projection method can be used to construct a good preconditioner for the generalized Stokes problem. Therefore, it is possible to solve iteratively the Stokes problem (33) in the spaces $\tilde{V}_h \times Y_h$ instead of using a projection scheme. Such an approach would be efficient at high Reynolds numbers or with small time steps.

4.2. A preconditioner for the mortar saddle point problem in three dimensions. Here we work in three dimensions, and we suppose that the partitioning into subdomains is regular and quasiuniform. We define by d_k the diameter of Ω_k and d an average diameter: there exists two constants C_1 and C_2 such that $C_1 d < d_k < C_2 d, \forall k \in \{1, \ldots K\}$. We also suppose for simplicity that the meshes in the subdomains are also regular and quasiuniform with constants and mean diameter independent of the subdomain. In particular, there exists two constants c_1 and c_2, such that for any $k \in \{1, \ldots K\}$ the diameter of the elements in Ω_k are greater than $c_1 h$ and smaller than $c_2 h$.

We consider the saddle point problem:

$$\begin{pmatrix} A & B^T \\ B & 0 \end{pmatrix} \begin{pmatrix} V \\ \Lambda \end{pmatrix} = \begin{pmatrix} F \\ 0 \end{pmatrix} \tag{47}$$

arising from the discretization by the mortar method of the elliptic equation

$$-\Delta p + \epsilon p = f \quad \text{in } \Omega, \tag{48}$$

$$\frac{\partial p}{\partial n} = 0 \quad \text{on } \partial\Omega \tag{49}$$

where ϵ is a positive parameter which may be taken as small as desired. Thus the Neumann problems in the subdomains are well posed. We use this equation as an approximation of the Poisson problem that is satisfied by the pressure, with $\epsilon = 10^{-4}$ or $\epsilon = 10^{-5}$.

The matrix A is a block diagonal matrix, each block corresponds to a discrete Neumann problem in Ω_k. The matrix B is the matrix of the jump bilinear form b_h in the nodal bases of X_h and $W_h \equiv \prod_{|\partial\Omega_l \cap \partial\Omega_k|>0} W_{k,l,h}$:

$$b_h(u_h, \mu_h) \equiv \sum_{k<l:\partial\Omega_l \cap \partial\Omega_k|>0} \int_{\Gamma_{kl}} (u_{kh} - u_{lh})\mu_{klh} \tag{50}$$

As proved in [**8**], the saddle point problem (47) enjoys a Babuška-Brezzi condition with an inf-sup constant independent on the parameter h. Therefore, (47) is well posed.

The preconditioned iterative algorithm described below has been proposed by Y. Kuznetsov in [**22**] and its parallel implementation has been fully described and tested in [**1**]. We assume that the subdomains have an aspect ratio bounded by a constant and that the coarse mesh is quasi uniform. Let $\mathcal{A}$ be a symmetric invertible matrix and let $\mathcal{B}$ be a symmetric and positive definite matrix. If the solutions of the generalized eigenvalue problem

$$\mathcal{A}X = \nu\mathcal{B}X$$

belong to the union of the segments $[d_1;\ d_2] \cup [d_3;\ d_4]$, where $d_1 \leq d_2 < 0 < d_3 \leq d_4$, the generalized Lanczos method of minimal iterations [**24**] for solving iteratively the system $\mathcal{A}X = F$, with the preconditioner $\mathcal{B}$ has a convergence rate depending on the generalized condition number $\kappa = \frac{\max\{d_4, |d_1|\}}{\min\{d_3, |d_2|\}}$.

Therefore, the idea is to use as a preconditioner for the saddle point problem (47) the matrix

$$\mathcal{B} = \begin{pmatrix} R_u & 0 \\ 0 & R_\lambda \end{pmatrix},$$

where R_u (resp. R_λ) is spectrally equivalent to A, (resp. $S_\lambda = BA^{-1}B^T$) (by spectrally equivalent, we mean that the condition number does depend neither on h, nor on the diameters of the subdomains nor on ϵ). For such a choice of $\mathcal{B}$, it can be proved that the generalized condition number κ does not depend on the parameters above. The matrices R_u and R_λ must also be chosen such that the systems $R_u v = w$ and $R_\lambda \mu = \beta$ are easy and inexpensive to solve.

It is natural to take R_u block diagonal with one block per subdomain: $R_u = diag(R_k)$ with the blocks R_k spectrally equivalent to the matrices A_k. Denote

$$\widehat{A}_k = \overset{\circ}{A}_k + \frac{1}{d^2} M_k, \tag{51}$$

where $\overset{\circ}{A}_k$ is the stiffness matrix (related to the Laplace operator with Neumann boundary condition in Ω_k), M_k is the mass matrix. Let P_k be the l_2 orthogonal projector onto the kernel of $\overset{\circ}{A}_k$, $\widehat{P}_k = I_k - P_k$ and H_k is any symmetric positive definite matrix spectrally equivalent to $\widehat{A}_k^{-1}$. Then, if R_k is chosen such that

$$R_k^{-1} = \widehat{P}_k H_k \widehat{P}_k + \frac{1}{\epsilon h^3} P_k, \tag{52}$$

it can be proved that R_k is spectrally equivalent to A_k [**22**]. It is for example possible to choose H_k as an additive multilevel preconditioner (see [**11, 31, 18**]), and this proves very efficient, since the cost of the matrix-vector product is proportional to the number of unknowns, and therefore optimal. The choice of the exponent 3 in the formula (52) is linked to the dimension and would have to be changed in dimension 2.

The construction of the preconditioner for S_λ consists of three stages:

- the first step consists of constructing a matrix $\widehat{S}_\lambda$ spectrally equivalent to S_λ such that the product of a vector by $\widehat{S}_\lambda$ is rather cheap;
- in the second step, a coarse grid preconditioner $\widehat{R}_\lambda$ is proposed for S_λ or equivalently for $\widehat{S}_\lambda$;
- in the third step, a generalized Chebyshev method with preconditioner $\widehat{R}_\lambda$ is applied to the matrix $\widehat{S}_\lambda$.

Let us call S_k the discrete Dirichlet to Neumann operator (Schur complement of the matrix A_k). The matrix $\widehat{S}_\lambda$ is chosen in the form

$$\widehat{S}_\lambda = \sum_{k=1}^{K} B_k \widetilde{H}_k B_k^T, \tag{53}$$

where B_k is the block of B corresponding with the degrees of freedom located on $\partial\Omega_k$, and where $\widetilde{H}_k$ is spectrally equivalent to S_k^{-1}: the matrix $\widetilde{H}_k$ is chosen as

$$\widetilde{H}_k = \widehat{P}_{\Gamma_k} \widehat{H}_{\Gamma_k} \widehat{P}_{\Gamma_k} + \frac{1}{\epsilon d h^2} P_{\Gamma_k}, \tag{54}$$

where P_{Γ_k} is the l_2 orthogonal projector onto the one dimensional space spanned by the vector of dimension n_{Γ_k} (n_{Γ_k} is the number of grid nodes on $\partial\Omega_k$) whose components are 1, $\widehat{P}_{\Gamma_k} = I_{\Gamma_k} - P_{\Gamma_k}$. The matrix $\widehat{H}_{\Gamma_k}$ is chosen to be spectrally equivalent to

$$\left(\overset{\circ}{S}_{\Gamma_k} + \frac{1}{d} M_{\Gamma_k} \right)^{-1},$$

where M_{Γ_k} denotes the $n_{\Gamma_k} \times n_{\Gamma_k}$ mass matrix on $\partial\Omega_k$ and where $\overset{\circ}{S}_{\Gamma_k}$ is the Schur complement of the matrix $\overset{\circ}{A}_k$.

The coarse space preconditioner $\widehat{R}_\lambda$ is defined as

$$\widehat{R}_\lambda = \sum_{k=1}^{K} D_k + \alpha B_{\Gamma_k} P_{\Gamma_k} {B_{\Gamma_k}}^T, \quad \alpha = \frac{1}{\epsilon d h^2}, \tag{55}$$

where D_k is a diagonal matrix, obtained by lumping the matrix $(1/h)B_{\Gamma_k}B_{\Gamma_k}{}^T$

It is proved in [**22**] that the condition number of $\widehat{R}_\lambda^{-1}\widehat{S}_\lambda$ can be bounded by cd/h where c is a positive constant independent of h, d and the small parameter ϵ.

Finally, the inverse of the preconditioner R_λ can be defined by

$$R_\lambda^{-1} = \left[I_\lambda - \prod_{l=1}^{L} \left(I_\lambda - \beta_l \widehat{R}_\lambda^{-1} \widehat{S}_\lambda \right) \right] \widehat{S}_\lambda^{-1}, \tag{56}$$

where I_λ is the $n_\lambda \times n_\lambda$ identity matrix (n_λ is the dimension of the space W_h), β_l are the Chebyshev parameters corresponding to the spectral bounds of $\widehat{R}_\lambda^{-1}\widehat{S}_\lambda$. If the number L of the preconditioned Chebyshev iterations is fixed to a value of the order $O(\sqrt{\frac{d}{h}})$, it can be proved that

$$R_\lambda \sim \widehat{S}_\lambda$$

thence,

$$R_\lambda \sim S_\lambda.$$

In order to have an optimal preconditioner in terms of arithmetical complexity, the matrix-vector product by $\widehat{S}_\lambda$ should be done in $O(d^{-\frac{1}{2}}h^{-\frac{5}{2}})$ operations at most. It is possible to construct such a matrix by noticing that, if $\widehat{H}_k$ is a matrix spectrally equivalent to the inverse of $\widehat{A}_k$, defined in (51), then the block of $\widehat{H}_k$, corresponding to the nodes located on the boundary of Ω_k, is spectrally equivalent to $(\overset{\circ}{S}_{\Gamma_k} + \frac{1}{d}M_{\Gamma_k})^{-1}$. For example, if $\widehat{S}_k$ is defined by using the Bramble Paschiak and Xu preconditioner [**11**] or the multilevel diagonal scaling preconditioner [**31**] then the global cost of the product by $\widehat{S}_\lambda$ is of order $O(\frac{1}{dh^2})$.

4.3. Numerical three dimensional experiments. The goal of this section is to demonstrate the very good parallel properties of the mortar element method and the block-diagonal preconditioner described above. Therefore we consider only uniform grids and decompositions into equal subdomains. The equation

$$-\Delta p + \epsilon p = f$$

with $\epsilon = 10^{-4}$ is solved in a parallelepiped. All the computations have been performed on the Cray T3E computer with up to 64 processors used. As a stopping criterion for the iterative method, we want to reduce the preconditioned residual by a factor η while the number of Chebyshev iterations is constant and equal to 8, except when mentioned explicitly. For all computations, the number of multigrid levels is equal to 4, except in section 4.3.1.

Note that even with matched grids at subdomains' interfaces the solution is different from that of the single domain case, because of the mortar element treatment of the interface.

4.3.1. *Computing time versus problem size.* The unit cube is decomposed into 64 cubic subdomains. In each subdomain the grid is uniform and contains N nodes, N taking the value 25^3, 33^3, 41^3. The total number of nodes varies from 1 000 000 to 4 410 944. The table 1 displays the dependence of the elapsed CPU time and of the number of iterations on N. The desired accuracy is 10^{-7} and the number of Chebyshev iterations is 8 or 16. For these tests, the number of multigrid levels equals 3, and the number of processors is fixed at 64.

TABLE 1. Number of iterations and elapsed CPU time *vs* the number of unknowns in the subdomains and the number of Chebyschev iterations, with 64 processors.

N		25^3	33^3	41^3
8 Cheb. it.	#iter	82	82	82
	T_{cpu}	39	81	141
16 Cheb. it.	#iter	66	68	68
	T_{cpu}	48	97	165

TABLE 2. CPU time (speed-up) *vs* the number of processors and stopping criterion.

Number of processors	16 4 sd./pr.	32 2 sd./pr.	64 1 sd./pr.	Number of iterations	$\|\|Bu^{k_\eta}\|\|$
$\eta = 10^{-5}$	89(1)	45(1.97)	23(3.86)	24	1.5e-5
$\eta = 10^{-6}$	247(1)	124(1.99)	64(3.85)	65	1.1e-6
$\eta = 10^{-7}$	351(1)	177(1.98)	91(3.85)	92	6.5e-8

The CPU time varies slightly sub linearly with the number of unknowns. This can be explained by cache effects when the size of the problem is increased.

4.3.2. *Computing time versus stopping criterion and number of processors.* In Table 2 the elapsed CPU time (in seconds) versus the stopping criterion ε and the number of processors is shown.

We wish to estimate the speed-up of the method, i.e. the dependence of the elapsed CPU time with the number of processors, the global mesh size of the problem and the number of subdomains being fixed. The total number of grid nodes is equal to $129 \times 129 \times 129 = 2\,146\,689$, and the number of subdomains is $4 \times 4 \times 4 = 64$. The subdomains are grouped into 16, 32 or 64 clusters ($N_c = N_c^x \times N_c^y \times N_c^z$), so that $16 = 4 \times 2 \times 2$ (4 subdomains per cluster), $32 = 4 \times 4 \times 2$ (2 subdomains per cluster), $64 = 4 \times 4 \times 4$ (1 subdomains per cluster). In the Table 2 the elapsed CPU time (in seconds) versus the stopping criterion η and the number of processors is shown. In the last column we give the Euclidean norm of Bu^{k_η}, which is nothing but the jump of the computed solution on the interfaces.

The actual speed-up, given in parentheses, is very close to the ideal, demonstrating thus very good parallel properties of the method. The speed-up is estimated with respect to the 16-processors case.

4.3.3. *Scalability.* The next series of results (Table 3) prove the excellent scalability of the algorithm. Now each subdomain is a cube with the edge length 0.5 and has a grid composed of $33 \times 33 \times 33$ nodes. The number of processors used for computation increases linearly with the number of subdomains, so that there is always one subdomain per processor. As we can see from the Table 3, the convergence rate is almost independent on the number of subdomains, although the boundary value problem is not the same, provided the grid in each subdomain does not change, and

TABLE 3. Number of iterations and CPU time *vs* the number of processors and stopping criterion for cubic subdomains.

N_{sd}		16	32	64
$\eta = 10^{-5}$	#iter	27	29	29
	T_{cpu}	23	27	28
$\eta = 10^{-6}$	#iter	43	45	46
	T_{cpu}	37	42	45
$\eta = 10^{-7}$	#iter	67	69	70
	T_{cpu}	58	63	69

TABLE 4. Effect of nonmatching grids.

	case 1	case 2
#iter	82	90
T_{cpu}	81	87

the CPU time increases less than 19%, when the number of processors goes from 16 to 64. This increase of CPU time can be explained by the fact that the average number of mortar sides per subdomain increases with the number of subdomains.

4.3.4. *Nonmatching uniform grids.* In this series of tests, we focus on the effect of nonmatching grids on the performances of the solver. The unit cube is divided into $4 \times 4 \times 4$ subdomains. We compare two cases: in the first case, all the subdomains have a grid with $33 \times 33 \times 33$ nodes, so the grids are matched at the interfaces. In the second case, only the subdomains located in the half space $x_3 > 0.5$ have $33 \times 33 \times 33$ nodes while the other subdomains have $25 \times 25 \times 25$ nodes. For these tests, the number of multigrid levels equals 3, and the number of Chebyshev iterations is 8.

The performances of the solver are slightly affected by the presence of nonmatching grids. In this example, the load balancing is very bad, so the CPU time is governed by the processors taking care of the finest grids.

5. Numerical results

5.1. 2D results. The 2D results presented here have been obtained with a characteristic Galerkin scheme, and a mortar element method. Here we have used the stream function-vorticity formulation, so the scheme is different from what has been described above, since the velocity is exactly divergence free. The linearized Stokes problem at each time step is computed by using a variant of the Glowinski-Pironneau algorithm see [**17, 2**].

Here we present simulations for the flow around a cylinder at Reynolds number 9500. This is a quite unsteady flow, which displays many structures. In Figures 1 and 2, we plot the vorticity at several times steps.

A part of the domain partition is plotted in the figure. The finite element used is an over parametric Q_1 element. The grids in the subdomain are structured and

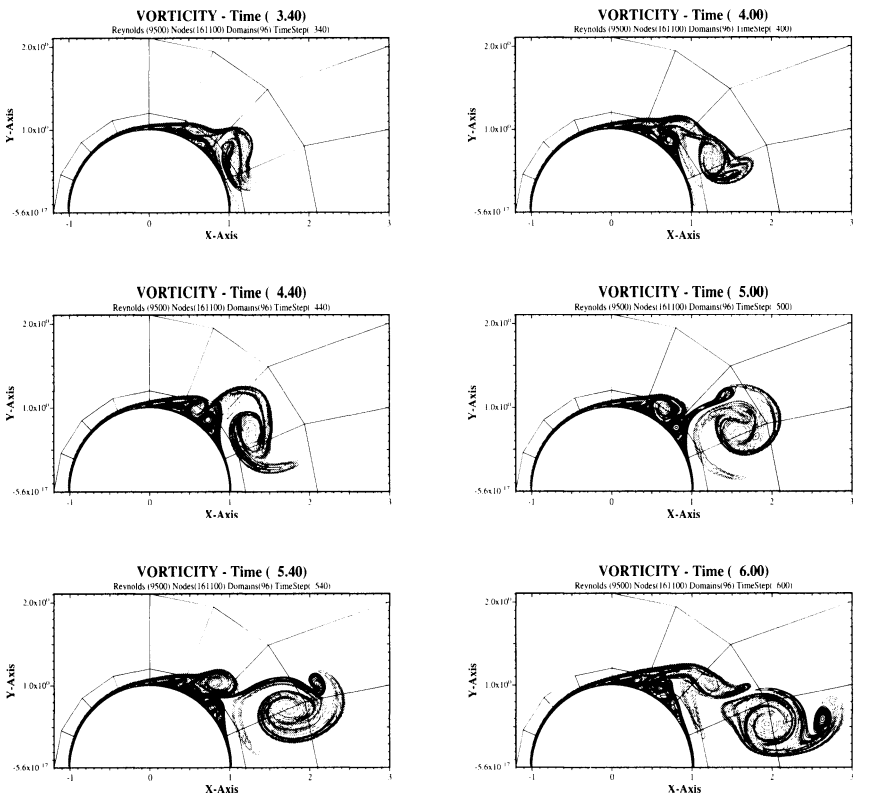

FIGURE 1. Flow around a cylinder at Reynolds number 9500 between t=3.4s and t=6s : zoom

refined with a geometrical progression near the walls. The global number of nodes is $\sim$ 160000 and the time step is 0.01. Although it is not seen, the meshes are not matched at the interfaces between the subdomains. However, the grids are fine enough so that there are no visible jumps.

The code is implemented with the parallel library PVM, and is not especially optimized. Such a computations takes two nights on a cluster of 8 HP9000 series700 workstations.

In Figure 3, we have plotted the drag coefficient as a function of time.

This coefficient is in good agreement with other computations [**21**].

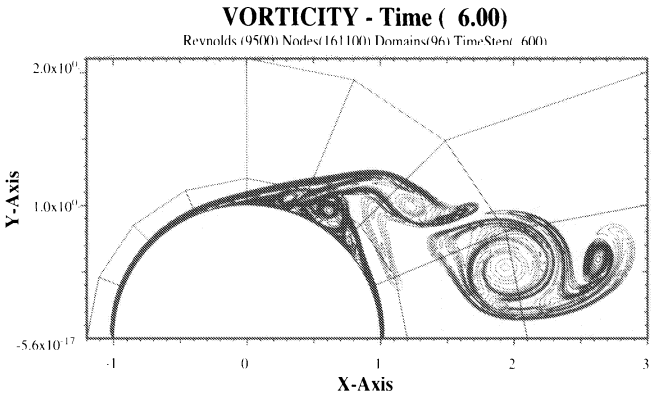

FIGURE 2. Flow around a cylinder at Reynolds number 9500 at time t=6s : zoom

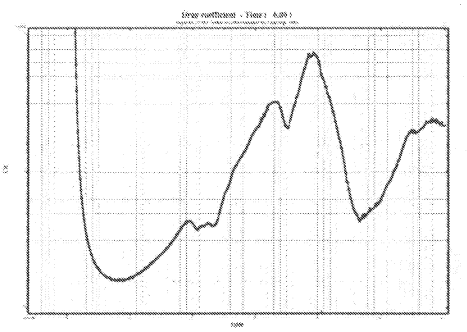

FIGURE 3. Flow around a cylinder at Reynolds number 9500: drag

5.2. 3D results.

5.2.1. *A lid driven cavity at Reynolds number 5000.* This test is concerned with a cubic lid driven cavity at Reynolds number 5000. The flow is driven at the upper wall, where its velocity is 1. On the other walls, a no-slip condition is imposed. The number of grid nodes is 2 100 000. The time step is 0.01. In Figure 4(left), we display the contour lines of the norm of the velocity in the cross-section $y = 0.5$. One can see two principal recirculations in the bottom of the cavity near the corners. The right part of the figure is a crossection in the cross-wind direction: $x = 0.766$. Here we see pairs of vortices in the bottom of the cavity: this instability is called the Taylor-Gortler instability. Note that, at this Reynolds number, this instability is highly unstationary.

The 3D code is written in C++ and parallelized with MPI. Therefore it has been possible to run it on several machines, *e.g.* PC with Linux, quadriprocessor HP9000, biprocessor Silicon Graphics, IBM SP2, Cray T3E. The present test has

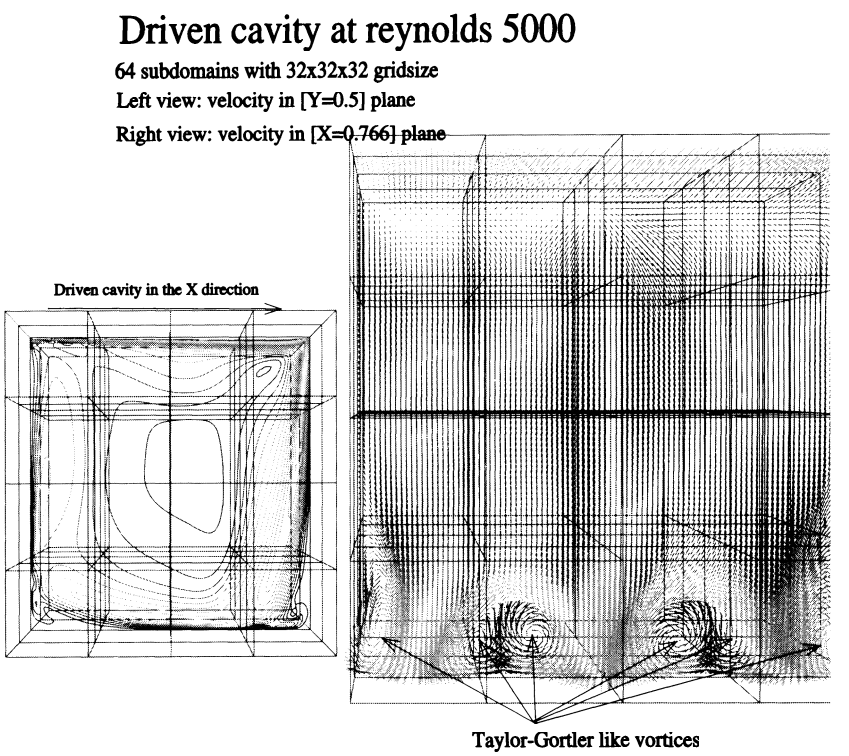

FIGURE 4. Flow in a driven cavity at Reynolds 5000: the Taylor-Gortler instability

been run on the Cray T3E at Idris(Orsay). One particularity of our code is that a single processor can handle several subdomains,

- for portability reasons.
- for load balancing: a discrete optimization algorithm is used to share the load and thus the subdomains between the processors in an optimal way.

There are 64 subdomains and 64 processors are used. Here the grids are matched, but the discretization is still non conforming, because no continuity is imposed at crosspoints and edges. For a single time step, (4 elliptic problems, the convection step, the computation of the gradient of the pressure, and the divergence of the velocity) it takes 55 s.

5.2.2. *Flow behind a cylinder at Reynolds number 20.* This test is concerned with the flow behind a cylinder at Reynolds number 20. There are 144 subdomains, (2 layers of 72 subdomains). We have displayed both the domain partition and the norm of the velocity on a crossection which lies at the interface between the two layers of subdomains: here, the continuity conditions are quite relaxed. However, the flow seems well computed even at the interface. To conclude, the computation seems correct though no quantitative tests have been done yet.

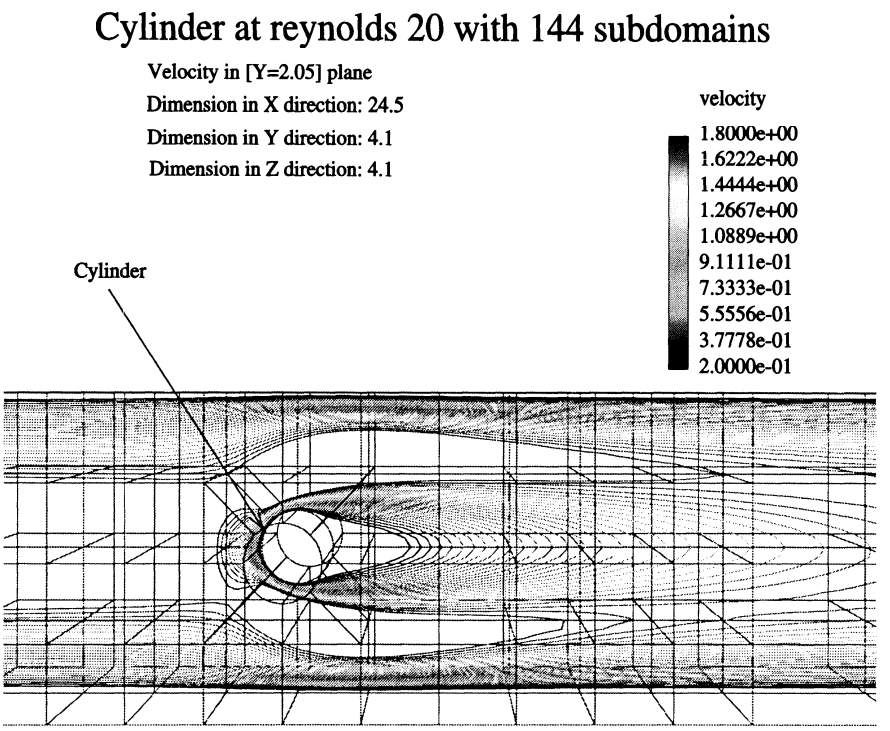

FIGURE 5. Flow behind a cylinder at Reynolds number 20

6. Conclusion

Discretization methods allowing nonmatching grids are useful for many reasons and in particular because they permit the use of locally structured grids. In this paper, we have presented two aspects of the use of nonmatching grids for computational fluid dynamics:

- We have shown how to modify the mortar method to deal with convection-diffusion problems
- We have presented a code in progress for the three dimensional incompressible Navier-Stokes equations.

The code is based on a characteristics-projection scheme, allowing us to use a fast solver developed in [**22**]. The tests presented above assess the efficiency of the scheme. We have presented also numerical results for high Reynolds flows in 2D and preliminary results in 3D. The results are correct despite the lack of strong continuity but quantitative tests remain to be done. These tests are not complete. In particular, we should investigate if mortar methods are still robust at high Reynolds number with rather coarse meshes, or if additional continuity constraints (continuity at edges or at crosspoints) should be added. We also plan to test the mortar method for compressible fluids.

References

1. G. Abdoulaev, Y. Achdou, Y. Kuznetsov, and C. Prud'homme, *On the parallel inplementation of the mortar element method*, (1997), To appear.
2. Y. Achdou and O. Pironneau, *A fast solver for Navier-Stokes equations in the laminar regime using mortar finite element and boundary element method*, SIAM J. Numer. Anal. **32** (1995), 985–1016.
3. Yves Achdou, *The mortar method for convection diffusion problems*, C.R.Acad. Sci. Paris, serie I **321** (1995), 117–123.
4. Yves Achdou and Jean-Luc Guermond, *Convergence analysis of a finite element projection/Lagrange-Galerkin method for the incompressible Navier-Stokes equations*, Tech. Report 96-19, LIMSI, LIMSI CNRS - BP 133 F-91403 ORSAY Cedex (France), December 1996.
5. Yves Achdou, Yvon Maday, and Olof B. Widlund, *Méthode itérative de sous-structuration pour les éléments avec joints*, C.R. Acad. Sci. Paris (1996), no. 322, 185–190.
6. G. Anagnostou, Y. Maday, C. Mavriplis, and A. Patera, *the mortar element method: generalization and implementation*, Proceedings of the Third International Conference on Domain Decomposition Methods for PDE (T. Chan et al, ed.), SIAM, 1990.
7. I. Babuška, *The finite element method with Lagragian multipliers*, Numer. Math. **20** (1973), 179–192.
8. Faker Ben Belgacem, *The mortar element method with Lagrange multipliers*, Université Paul Sabatier, Toulouse, France, 1994.
9. C. Bernardi and Y. Maday, *Raffinement de maillage en éléments finis par la méthode des joints*, C.R. Acad. Sciences, Paris, t 320, serie I, **320** (1995), 373–377.
10. Christine Bernardi, Yvon Maday, and Anthony T. Patera, *A new non conforming approach to domain decomposition: The mortar element method*, Collège de France Seminar (Haim Brezis and Jacques-Louis Lions, eds.), Pitman, 1994, This paper appeared as a technical report about five years earlier.
11. James H. Bramble, Joseph E. Pasciak, and Jinchao Xu, *Parallel multilevel preconditioners*, Math. Comp. **55** (1990), 1–22.
12. F. Brezzi, *On the existence, uniqueness and approximation of saddle point problems arising from Lagrangian multipliers*, R.A.I.R.O. Anal. Numér. **8** (1974), 129–151.
13. J. Cahouet and J.P. Chabard, *Some fast 3-D finite element solvers for generalized Stokes problems*, Int. J. Num. Meth. in Fluids **8** (1988), 269–295.
14. Mario A. Casarin and Olof B. Widlund, *A hierarchical preconditioner for the mortar finite element method*, ETNA **4** (1996), 75–88.
15. A. J. Chorin, *On the convergence of discrete approximations to the Navier–Stokes equations*, Math. Comp. **23** (1969), 341–353.
16. Maksymilian Dryja, *A substructuring preconditioner for the mortar method in 3d*, these proceedings, 1998.
17. R. Glowinski and O. Pironneau, *Numerical method for the first biharmonic equation and for the Stokes problem*, SIAM review **21** (1974), 167–212.
18. M. Griebel, *Multilevel algorithms considered as iterative methods on semidefinite systems*, SIAM J. Sci. Comput. **15** (1994), 604–620.
19. J.L. Guermond, *Some implementations of projection methods for Navier–Stokes equations*, Modél. Math. Anal. Numér. (M^2AN) **30** (1996), 637–667.
20. C. Johnson, U. Navert, and J. Pitkaranta, *Finite element method for linear hyperbolic problems*, Comp. Meth. in Appl. Eng. **45** (1984), 285–312.
21. P. Koumoutsakos and A. Leonard, *High resolution simulations of the flow around an impulsively started cylinder using vertex methods*, J. Fluid. Mech. **296** (1995), 1–38.
22. Yuri A. Kuznetsov, *Efficient iterative solvers for elliptic finite element problems on nonmatching grids*, Russ. J. Numer. Anal. Math. Modelling **10** (1995), 187–211.
23. Patrick Le Tallec, *Neumann-Neumann domain decomposition algorithms for solving 2D elliptic problems with nonmatching grids*, East-West J. Numer. Math. **1** (1993), no. 2, 129–146.
24. G.I. Marchuk and Y.A. Kuznetsov, *Méthodes itératives et fonctionnelles quadratiques*, Méthodes Mathématiques de L'Informatique : Sur les Méthodes Numériques en Sciences, Physiques et Economiques (G.I. Marchuk J.L. Lions, ed.), vol. 4, Dunod, Paris, 1974.
25. O. Pironneau, *On the transport diffusion algorithm and its application to the Navier–Stokes equations*, Numer Math **38** (1982), 309–332.

26. R. Rannacher, *On Chorin's projection method for the incompressible Navier–Stokes equations*, Lectures Notes in Mathematics, vol. 1530, Springer, Berlin, 1992, pp. 167–183.
27. E. Suli, *Convergence and nonlinear stability of the Lagrange-Galerkin method*, Numer Math **53** (1988), 459–483.
28. P. Le Tallec, T. Sassi, and M. Vidrascu, *Domain decomposition method with nonmatching grids*, Proceedings of DDM 9, AMS, 1994, pp. 61–74.
29. R. Temam, *Une méthode d'approximation de la solution des équations de Navier–Stokes*, Bull. Soc. Math. France **98** (1968), 115–152.
30. Stefan Turek, *Multilevel pressure-Shur complement techniques for the numerical solution of the incompressible Navier–Stokes equations*, Habilitation thesis, Institut fur Angewandte Mathematik, Universitat Heidelberg Im Neuenheimer Feld 294 69210 Heidelberg Germany, 1996, email:ture@gaia.iwr.uni-heidelberg.de.
31. X.Zhang, *Multilevel Schwarz methods*, Numer Math **63** (1992), 521–539.

INSA Rennes, 20 Av des Buttes de Coesmes, 35043 Rennes, France
E-mail address: yves.achdou@insa-rennes.fr

Institute of Numerical Mathematics, Russian Academy of Sciences, Ul. Gubkina 8, GSP-1,Moscow, Russia
Current address: CRS4, Via N. Sauro 10, Cagliari 09123, Italy
E-mail address: gassan@crs4.it

Université Paris 6, Analyse Numérique, 75252 Paris cedex 05, France

University of Houston, Department of Mathematics, Houston, Texas and Institute of Numerical Mathematics, Russian Academy of Sciences, Moscow 117334, Russia
E-mail address: kuz@math.uh.edu

Université Paris 6, Analyse Numérique, 75252 Paris cedex 05, France
E-mail address: pironneau@ann.jussieu.fr

Laboratoire ASCI, Batiment 506, 91403 Orsay, France
E-mail address: prudhomm@asci.fr